Journal of Regenerative Medicine

Research Article

A SCITECHNOL JOURNAL

Human Mesenchymal Stem Cells seeded in 3D Collagen Matrix Scaffolds as a Therapeutic Alternative in Tissue Regeneration

Benjamin León-Mancilla[1,5], Moisés Martínez-Castillo[1], Rocio Guerrero-Bustos[2], Juan J Montesinos[3], Erika Hernández-Estévez[3], Zaira Medina-Avila[1], Maria Cristina Piña-Barba[4], Rubén S Argüero[5], Gabriela Gutierrez-Reyes[1]*

Abstract

Human mesenchymal stem cells (hMSCs) are considered an ideal strategy for tissue engineering and regenerative medicine. However, their acquisition, administration route, and cell quantity are true challenges. On the other hand, the collagen scaffolds are a viable option, mimicking the extracellular matrix, utilizing collagen as the main polymer in 3D supports. The combination of hMSCs and scaffolds could enable the hMSCs to arrive at the target organ, avoiding the disadvantages of intravenous or intra-arterial therapy. We obtain and characterize MSCs from human amniotic membranes and evaluate their differentiation capacity in 3D collagen matrix scaffolds (CMSs). Their morphology, multipotency genes by RT-PCR and markers by flow cytometry were evaluated in in vitro cell cultures. The differentiation capacity of AM-hMSCs, seeded with and without CMSs, was evaluated in media specific for chondrogenic, osteogenic, and adipogenic lineages. AM-hMSCs were studied up to passage 5 and fibroblastoid morphology was observed in AM-hMSCs and BM-hMSCs. sox-2 gene expression was similar in all passages, whereas oct-4 was upregulated at P2 and P5. Nanog was upregulated at P1 and P3 versus BM-hMSCs. Membrane markers displayed CD44, CD73, CD90, and CD105 were positive in all passage. AM-MSCs were adhered to CMSs, showing fibroblastoid morphology in the SEM analyses. The AM-hMSCs, seeded with and without CMSs, were able to differentiate into chondroblasts, osteoblasts, and adipocytes. The CMSs enable AM-hMSCs stemness preservation, without affecting their differentiation capacity. That combination can be a novel strategy in the tissue regeneration process.

Keywords

Mesenchymal stem cells, Collagen matrix scaffolds, Tissue regeneration, Xenogenic construct

Introduction

Chronic noncommunicable diseases, such as cardiovascular diseases, cancer, renal failure, respiratory diseases, diabetes, and chronic liver diseases, have been increasing in recent years, affecting quality of life and life expectancy [1]. Organ transplantation is usually the only alternative in patients with complications, but only 10% of those patients are transplanted, mainly due to the scarcity of organ donation and elevated preoperative and postoperative costs [2,3]. SARS-CoV-2 infection has also become a novel challenge in solid organ transplantation [4,5]. In 1993, Langer and Vacanti proposed tissue engineering (TE) and regenerative medicine (RM) as alternatives to transplantation. The primary components of TE include the use of cells (with multi or pluripotency), scaffolds (biomaterials), and growth factors. Mesenchymal stem cells (MSCs) are stem cells of choice in TE [6-8]. The main source of MSCs is bone marrow, but their procurement involves a complex procedure that is invasive and painful [9]. The placenta is considered biologic waste. However, that organ has specific sites for MSCs procurement, such as the amniotic membrane (AM), umbilical cord blood (UCB), Warthon gelatin (WG), cotyledons, and amniotic fluid. In in vitro studies, AM-hMSCs have been reported to possess a high capacity to differentiate into ectoderm, mesoderm, and endoderm lineages [10,11].

Scaffolds used in TE and RM include either natural or synthetic materials that must have the biologic characteristics of biocompatibility, biodegradability, and the capacity to induce MSCs differentiation into selected lineages, through the incorporation of specific growth factors [12]. Natural scaffolds designed from collagen have demonstrated synergy with hMSCs in the process of tissue regeneration [13]. However, collagen scaffolds are obtained through chemical processes involving the tendons, pericardium, intestine, and dermis [14]. In contrast, our group previously reported that the collagen matrix scaffold (CMS), obtained from bone, taking advantage of the 3D composition (porous structure), was used as an experimental scaffold. The results showed that the implantation of CMSs in the urethra and bile duct promoted regeneration and restored function in preclinical studies [15,16]. Nevertheless, the combination of MSCs and biomaterials has been suggested as an excellent option for improving organ damage. There are no studies that focus on the interaction of AM-hMSCs and CMSs [17]. Thus, we evaluated and characterized the combination of AM-hMSCs and CMSs in vitro, suggesting their potential as a therapeutic strategy in the regeneration of several tissues.

Materials and Methods

Patients

To obtain the hMSCs from the amniotic membrane (AM), 30 women, ranging from 20 to 30 years of age that presented with no clinical complications during the gestation period were included in the study. The exclusion criteria were systemic infections and comorbidities (e.g., diabetes, hypertension, and autoimmune diseases), as well as patients with positive serologic test results for the hepatitis A, B, and C viruses and HIV. A detailed clinical history of previous pregnancy conditions (natural childbirth, abortions, and cesarean sections) was documented. The maternal anthropometric

***Corresponding author:** Gabriela Gutierrez-Reyes, Liver, Pancreas and Motility (HIPAM) Laboratory; Unit of Experimental Medicine; School of Medicine, Universidad Nacional Autónoma de México, UNAM. Hospital General de México, School of Medicine, Universidad Nacional Autónoma de Mexico (UNAM), Hospital General de México, Dr. Balmis 148. Doctores, Cuauhtémoc, Mexico City, 06726, Mexico; E-mail: gabgurey@yahoo.com.mx

Received: June 28, 2021 **Accepted:** July 19, 2021 **Published:** July 26, 2021

information included age, height, weight, body mass index (BMI), alcohol consumption, and smoking habit. The neonatal information was also registered (sex, Apgar score, and placental weight). All participants provided written statements of informed consent. The present study was approved by the research and ethics committees of the Hospital General de México "Dr. Eduardo Liceaga" (CI/315/15) and the School of Medicine at the Universidad Nacional Autónoma de México (DI/115/2015) and was conducted in accordance with the principles described in the 1975 Declaration of Helsinki.

Isolation of hMSC$_s$ from the Placenta

The AM-hMSCs were obtained from placentas from natural deliveries or cesarean sections, as previously reported [18]. Briefly, a 5-8 cm section was carefully taken from the AM during childbirth. The samples were washed twice with an antibiotic-antimycotic (Gibco, Grand Island, NY, USA) in PBS, after which the AM was cut into small pieces in 0.05% Trypsin-EDTA (Gibco, Grand Island, NY, USA), and the tissue was stored at 37°C for 60 min. Enzymatic digestion was carried out using collagen type II (Gibco, Grand Island, NY, USA) at 37° for 90 min. Finally, the cells were cultured at 37°C at 5% CO2 in Dulbecco's Modified Eagle Medium (DMEM) (Gibco, Grand Island, NY, USA), supplemented with 10% FBS (Biowest, France), 1% antibiotic-antimycotic (Gibco, Grand Island, NY, USA), (3.7 g/L) sodium bicarbonate (Sigma Aldrich, Germany), and (1M) HEPES (Sigma Aldrich, Germany). Positive control of the bone marrow (BM) hMSCs was provided by the Mesenchymal Stem Cell Laboratory of the Oncology Disease Medical Unit of the Instituto Mexicano del Seguro Social (IMSS) in Mexico.

AM-hMSCs Characterization

Morphology: The morphology of placental AM-hMSCs was evaluated at different culture times. The cells were maintained until reaching 80 to 90% confluency (approximately 2 weeks). The trypsinization process was performed, considering it the first passage (P1). The cultures from different passages (1, 2, 3, 4, and 5) were viewed, using a Nikon Eclipse TE 2000-S (Tokyo, Japan) inverted microscope and hMSC**s** morphology was evaluated by Differential Interface Contrast (DIC/Nomarski). Briefly, 2x10^4 cells from passage 3 that had previously been placed in 24-well cell culture clusters (Corning, New York, USA) with DMEM, were seeded onto sterile cover glasses (Marienfeld, Germany) (16 mm Ø). The cells were evaluated after 15 days of cell culture (Nikon Microphoto FDA, camera Nikon DMX; Tokyo, Japan). Three independent experiments were performed for each cell passage.

Multipotential gene expression in AM-hMSCs

To evaluate genes related to MSCs multipotency, we performed RNA extraction, using a Trizol reagent (Thermo Fisher Scientific, Waltham, MA, USA). AM-hMSCs RNA at passages 1-5 (n=3) were precipitated by isopropanol (1 mL). The RNA pellet was then collected and precipitated with 75% ethanol, centrifuged at 12,000 r/min, and resuspended with (40 µL) of RNase-free water. Afterwards, cDNA synthesis was performed using Reverse Transcription Polymerase Chain Reaction (Thermo Fisher Scientific, Waltham, MA, USA) for (2 ug) to the total RNA, using the AMPLIQON kit (Odense, Denmark).

Multipotential gene primers were designed, using the NIH Gen Bank database. The primers used were: sox-2 (167bp), forward 5′-CCCCCGGCGGCAATAGCA-3′, reverse5-′TCGGCGCCGGGGAGATACAT-3′; for oct-4 (125bp), forward 5′-TCGAGAACCGAGTGAGAGG-3′, reverse 5-GAACCACACTCGGACCACA-3′, nanog (481bp) forward 5′TTGTGGGCCTGAAGAAAACTATCC 3′, reverse 5 ′CTGCGTCACACCATTGCTATTCTT-3′; and gapdh (598bp), forward 5′-CTCTTGCTCTCAGTATCCTTG-3′, reverse 5′-GCTCACTGGCATGGCCTTCCG-3′. PCR was carried out with a Veriti Thermal Cycler (Thermo Fisher Scientific, Waltham, MA, USA), maintaining the following conditions: for sox-2: 35 cycles, denaturation 95°C, annealing at 56.9 °C for 45 s, and extension at 72°C for 30 s; for oct-4: 35 cycles, denaturation 95°C, annealing at 60°C for 45 s, and extension at 72°C for 30 s; for nanog: 35 cycles, denaturation 95°C, annealing at 57.6 °C for 45 s, and extension at 72°C for 30 s; and for gapdh as the housekeeping gene: 35 cycles, denaturation 95°C for 5 s, annealing at 60°C for 45 s, and extension at 72°C for 30 s. The sox-2 and oct-4 PCR products were separated into 3% (w/v) agarose gels, whereas the nanog and gapdh products were separated into 1.5% (w/v) gels, which were stained with ethidium bromide and viewed on a Kodak UV transilluminator (Rochester, NY, USA).

AM-hMSCs Immunophenotype Characterization

The AM-hMSCs membrane immune markers were analyzed by flow cytometry. The AM-hMSCs from the different cell passages were trypsinized and adjusted at 4 x 10^4. The cells were evaluated, using the human MSCs analysis kit (BD Biosciences, Franklin Lakes, NJ, USA), following the supplier's recommendations. Briefly, the samples were incubated for 30 min at room temperature with fluorescein isothiocyanate (FITC)-conjugated anti-CD90, phycoerythrin (PE)-conjugated anti CD44, peridinin chlorophyll protein (PerCP-Cy 5.5)-conjugated anti-CD105, and allophycocyanin (APC)-conjugated anti CD73 antibodies, as multipotential markers, whereas negative immunophenotype markers were determined using phycoerythrin (PE)-conjugated anti CD34, CD11b, CD45, CD19, and HLA-DR. The BM-hMSC immunophenotype characterization was used as a positive control. We analyzed 20,000 events in a FACSCanto II flow cytometer and the data were processed using the FACSDiva software package (BD Biosciences, Franklin Lakes, NJ, USA). Three independent experiments were performed for each cell passage.

Assays for AM-hMSCs differentiation specific phenotypes

The differentiation of AM-hMSCs into chondrogenic, osteogenic, and adipogenic phenotypes was assessed at day 21. We seeded 4 x 10^4 cells in culture dishes (3 mm) (Corning Costar, New York, NJ, USA), using the previously reported specific differentiation media [19] Differentiation was induced with a chondrogenic medium (Cambrex Bio Science, NJ, USA) supplemented with transforming growth factor-β (Cambrex Bio Science, NJ, USA). The osteogenic and adipogenic media were acquired from Stem Cells Technology (Vancouver, BC, Canada). The osteogenic medium was supplemented with ascorbic acid and β-glycerolphosphate and the adipogenic medium was supplemented with premix ITS (Stem Cell Technologies Inc., Vancouver, BC, Canada). Finally, the cell cultures were evaluated using Alcian blue (Sigma-Aldrich, St. Louis, MO, USA) for the differentiation into the chondrogenic lineage and the von Kossa stain for the differentiation into the osteogenic phenotype. The lipid vacuoles were stained with red-O oil (Sigma-Aldrich, Germany) for the adipogenic differentiation. Images were obtained by light microscopy, using Nikon Microphoto FDA, a Nikon DMX camera, and Nikon ACT software (Tokyo, Japan). Three independent experiments were performed for each cell passage.

Collagen Matrix Scaffold (CMS) obtainment

The biomaterial was obtained from bovine femoral epicondyles, treated with hydrochloric acid to eliminate mineral components. The scaffolds were physically and chemically characterized, establishing collagen type I as the main component. The CMSs has open pores of different sizes that facilitate the interchange of fluids and other components, such as growth factor [20] and it can also be designed in different geometries, according to the implanted organ [15,16].

Characterization of the AM-hMSCs seeded in CMSs

To determine the multipotential ability of AM-hMSCs in vitro, the cells were seeded in CMSs. Before seeding the cells onto the scaffolds (14 mm of diameter and 1 mm of thickness), they were hydrated for 24 hours in DMEM (1ml) at 37°C in 24-well cell culture clusters (Corning Costar, New York, NJ, USA). A total of $1x10^5$AM-hMSCs were added to the CMSs, with DMEM as the control, and they were then incubated with the abovementioned differentiation media (chondrogenic, osteogenic and adipogenic) at days 14 and 21. The media (1 ml) were changed every 3 days. To evaluate the differentiation of the AM-hMSCs and their attachment to the CMSs, the samples were fixed in 10% formalin and embedded in paraffin. The AM-hMSCs with the CMSs were stained with hematoxylin and eosin (H&E), and the specific stain of each of the three lineages was performed with the same technique used in the differentiation assays. Images were obtained by light microscopy (Nikon, Tokyo, Japan). To evaluate the morphology and adhesion of the AM-hMSCs in the CMSs at days 14 and 21, we employed SEM. In brief, the samples were washed with sterile PBS and fixed with Zamboni fixative solution (Newcomer supply, Middleton, WI, USA) for 24 h. The samples were then processed [21] and covered with conductive material (Au). The samples were evaluated utilizing DSM-950 and Evo10 electron microscopes (Zeiss, Oberkochen, Germany).

Statistical analysis

Comparisons between groups were performed with the one-way ANOVA analysis and Tukey-Kramer post-hoc test. Data were expressed as mean ± standard error. A p value < 0.05 was considered statistically significant. Statistical analyses were performed using SPSS 20.0 software (IBM, Armonk, NY, USA).

Results

Patients

A total of 30 amniotic membranes from female patients were included. The patients were divided into two age groups (20 to 25-year-olds and 26 to 30-year-olds), as previously reported [22]. Fifty-seven percent of the patients were 20-25 years of age and 43% were 26-30 years of age. Patient overweight was similar in the two subgroups, with a BMI of 26.5 kg/m^2 for the 20 to 25-year-olds and 26.9 kg/m^2 for the 26 to 30-year-olds. The obese 20 to 25-year-olds had a BMI of 35.4 kg/m^2 versus 34 kg/m^2 in the 26 to 30-year-olds. We obtained more placentas via natural delivery (22 patients), compared with cesarean section (8 patients). The demographic and gynecologic data are shown in Table 1.

AM-hMSCs morphology and cell culture

The representative portion of the AM was obtained from the placenta (Figure 1A). The tissue was processed and the MSCs were maintained in vitro. The attached cells had a circular shape at 2 h of culture (Figure 1B). After 14 days, the culture cells had proliferated and presented with lamellipodia morphology, as well as triangular, rhomboidal, and fibroblast-like morphology types (Figure 1C). The morphology of the cultured BM-hMSCs at 2 h and at day 14 was similar to that of the AM-hMSCs (Figure 1D and E). Additionally, the DIC/Nomarski evaluation revealed the integrity of cell nuclei and the cytoskeletal arrangement of the AM-hMSCs (Figure 1F-G).

Multipotential Gene Expression in AM-hMSCs

After evaluating the AM-hMSC morphology, we determined the expression of the multipotential genes: sox-2, nanog, and oct-4. Representative agarose gels revealed the expected sox-2, oct-4, nanog, and gapdh products at 167pb, 125pb, 481pb, and 598pb, respectively, in passages P1 to P5 (Figure 2A, C, E, and G). The densitometric analysis of sox-2 revealed no statistical differences at any passage evaluated. However, its relative expression was lower in the AM-hMSCs, compared with the BM-hMSCs (Figure 2B). On the other hand, the expression of oct-4 in P2 and P5 of the AM-hMSCs displayed statistically significant differences from the BM-hMSCs ($p< 0.05$) (Figure 2D), whereas the expression of nanog was higher in passages P1 to P3 than in passages P4 and P5, in both the AM-hMSCs and the BM-hMSCs ($p<0.05$) (Figure 2F). The expression of gapdh as a housekeeping gene presented no differences in P1 to P5 (Figure 2H).

Immunophenotype Characterization of AM-hMSCs

To perform the immunologic characterization of the AM-hMSCs, we evaluated CD44, CD73, CD90, and CD105 as positive markers of MSCs and CD34, CD11b, CD45, CD19, and HLA-DR as negative markers, by FACS. The cytometric analysis revealed that CD44+ presented no differences in its expression at P1 to P5, in either the AM-hMSCs or the BM-hMSCs (Figure 3A). The percentage of CD73+ in the AM-hMSCs from P1 to P5 was approximately 89%, with similar results in the BM-hMSCs (94%) (Figure 3B). Likewise, the percentage of CD90+ was maintained at 90% in all the AM-hMSCs passages and at 96% for the BM-hMSCs (Figure 3C). Interestingly, the CD105+ marker had lower expression in the AM-hMSCs at P1 (60%) and at P2 to P5 (24%), in comparison with the BM-hMSCs (75%) ($p<0.05$) (Figure 3D). The evaluation of the CD34, CD11b, CD45, CD19, and HLA-DR mixed hematopoietic stem cell markers was less than 14% in the AM-hMSCs at all passages evaluated and that phenotype was similar in the BM-hMSCs (Figure 3E). All data are summarized in Table 2.

Assays for AM-hMSCs differentiation into specific phenotypes

After evaluating the morphology and genotypic and immunologic characterizations, we determined the capacity of AM-hMSCs to differentiate into chondroblast, osteoblast, and adipocyte lineages. The results showed that approximately 80% of the AM-hMSCs from P2 to P5 were positive for the Alcian blue stain, revealing the chondroblast lineage (Figure 4A). Similarly, 80% of AM-hMSCs were positive for the von Kossa stain and the osteoblasts showed calcium deposition and changes in their morphology (Figure 4B). The adipocytes stained with red-O oil revealed lipid vacuoles in approximately 25% of cells in all passages (Figure 4C). The percentage of each differentiation is shown in Table 3.

Characterization of AM-hMSCs seeded in Collagen Matrix Scaffolds

The SEM results confirmed the fibroblastoid morphology and the high capacity of AM-hMSCs to adhere at the rough surface of

		BMI (%)		Delivery (%)	
Patients	**Age (%)**	**Overweight**	**Obesity**	**Natural**	**Cesarean**
30	20-25 (57)	26.5 (23.3)	35.4 (33.3)	13 (43.3)	4 (13.3)
	26-30 (43)	26.9 (16.6)	34 (26.6)	9 (30)	4 (13.3)
BMI: Body Mass Index					

Table 1: Patient demographic and gynaecologic data overweight.

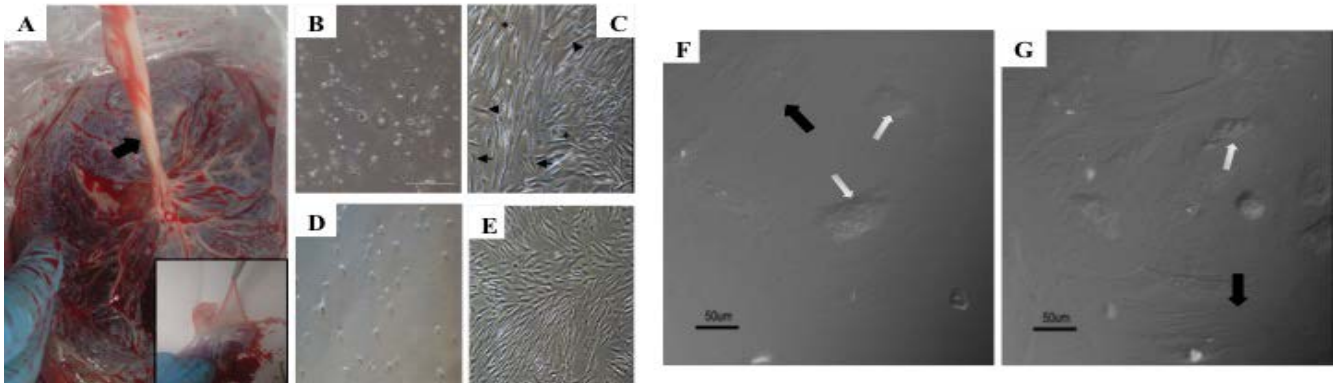

Figure 1: Obtention and morphology of AM-hMSCs. A. A 5-8 cm AM was selected to obtain AM-hMSCs, umbilical cordon as reference (arrow). B. AM-hMSCs culture after 2 h of obtention, displays circular shape. C. Culture at 14 d of AM-hMSCs showed lamellipodia (arrowhead), triangle (arrow), rhomboid (asterisk) and like-fibroblast morphology. D-E. Culture of BM-hMSCs after 2 h and 14 days of obtention were a positive control. F-G. DIC/Nomarski analysis showed AM-MSCs nucleus (white arrow) and cytoplasm (black arrow). B-E: 4x. F-G: 20x.

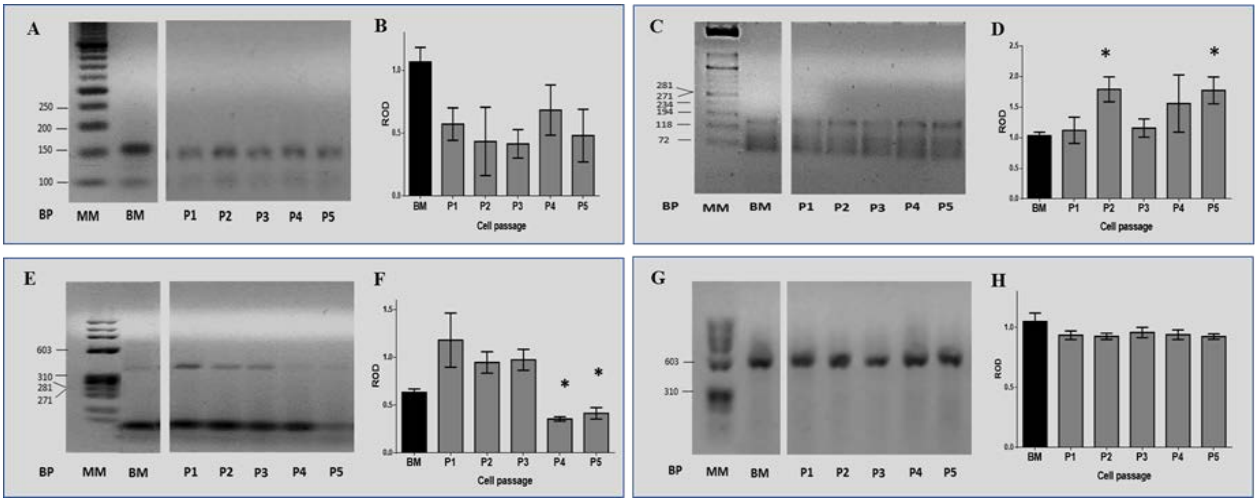

Figure 2: Expression of multipotent genes in AM-hMSC. A-B. sox-2 is present in passage P1 to P5, not show different with the BM-MSCs. C-D. oct-4 not show different in all passage and not have different with BM-MSCs. E-F. nanog show similar concentration in P1-P3 but different in P4-P5 that have differences with BM-MSCs. G-H. gapdh used to housekeeping. A: 50bp (DNA step Ladder, Sigma-Aldrich); C, E and G: 100bp (ϕX174DNA, Thermo-Scientific) *p<0.05.

the CMSs (Figure 5A). Additionally, we observed the lamellipodia morphology of AM-hMSCs at day 14 (Figure 5B). Furthermore, the AM-hMSCs with CMSs released spherical microvesicles, or perhaps "exosomes", at day 21 (Figure 5C).

The differentiation capacity of AM-hMSCs in the CMSs, with or without specific differentiation media, demonstrated that the distribution and percentage of cells adhered to CMSs were similar at days 14 and 21. The cells with no differentiation media were stained with H&E (Figure 6A and B). The chondrogenic differentiation of AM-hMSCs in CMSs showed that approximately 50% of cells were positive for the Alcian blue stain (Figure 6C and D). Similar behavior was observed in the osteogenic differentiation in the CMSs (Figure 6E and F). In the specific medium for adipocyte differentiation, only 5-7% of cells were positive for the red-O oil stain. Those cells showed the peripheral nuclei, which are a typical characteristic of that lineage (Figure 6G and H).

The data obtained in the characterization assays support the concept that AM-hMSCs conserve viability, adhesive capacity, and differentiation capacity. The AM-hMSCs, seeded with and without CMSs, maintained those properties in the scaffolds from the xenogenic source.

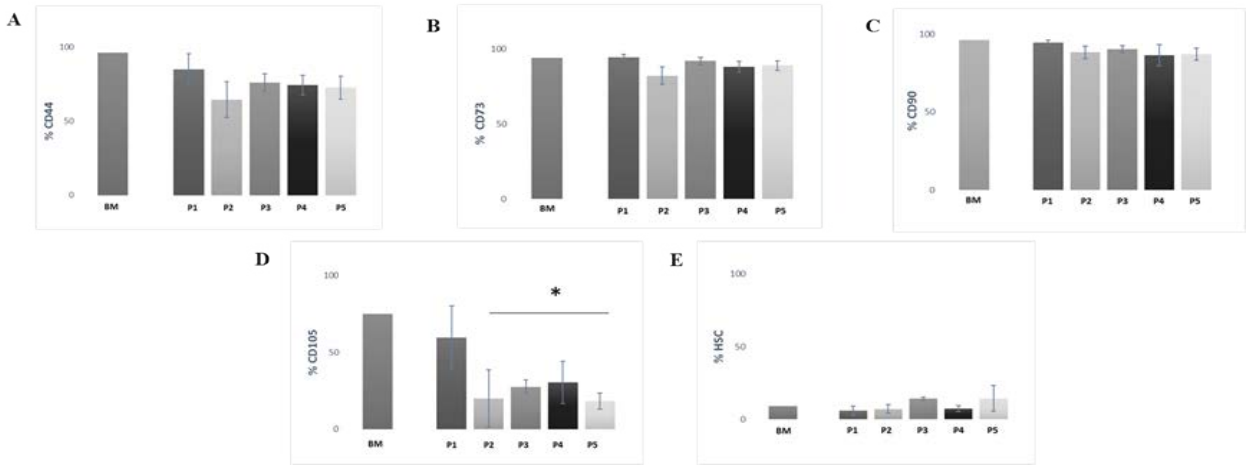

Figure 3: Immunophenotype characterization of AM-hMSCs. A. Percentage of CD44+ not presented differences in all passage with respect BM. B. CD73+ percentage is similar AM and BM-hMSCs in all passage. C. CD90+ was similar in AM-hMSCs with respect BM-hMSCs in P1 and P3. D. CD105+ was lower in all passage compared with BM-hMSCs. E. Negative markers were low in all passage in AM-hMSCs and BM-hMSCs. *p<0.05 (BM vs P2-P5 CD105+).

	%					
Markers	**P1**	**P2**	**P3**	**P4**	**P5**	**MO**
CD44	85 ± 15	64 ± 21	76 ± 15	67 ± 12	73 ± 17	96
CD73	94 ± 1	82 ± 10	92 ± 6	88 ± 10	89 ± 7	94
CD90	94 ± 3	88 ± 7	90 ± 5	86 ± 18	87 ± 9	96
CD105	60 ± 18	20 ± 33	28 ± 11	30 ± 38	18 ± 12	74
Negative	6 ± 7	7 ± 5	14 ± 11	7 ± 6	14 ± 20	9

Table 2: Percentage for positive and negative markers in different passage.

Negative markers: CD34, CD45, CD11B, CD19, HLA-DR

Three independent experiments were performing for each cell passages.

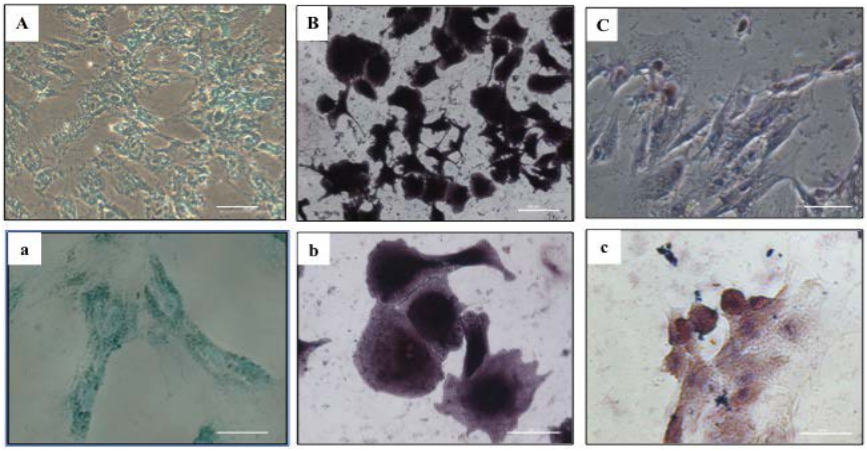

Figure 4: Differentiation potential of AM-hMSCs into chondroblasts, osteoblasts and adipocytes. A-a. Formation of proteoglycans in chondroblasts were stained with Alcian blue. B-b. Calcium depositions in osteoblasts were stained with von Kossa. C-c. In adipocytes the formation of lipids droplets were stained with oil red O. A-C: 4x, a-c: 20x.

Passage	**Chondrogenic potential**	**Osteogenic Potential**	**Adipogenic Potential**
2	80 ± 10	80 ± 10	30 ± 5
3	70 ± 17	90 ± 8	30 ± 7
4	80 ± 17	80 ± 14	20 ± 10
5	75 ± 15	80 ± 15	15 ± 6

Table 3: AM-hMSCs differentiation percentage in different passage.

Three independent experiments were performing for each cell passage

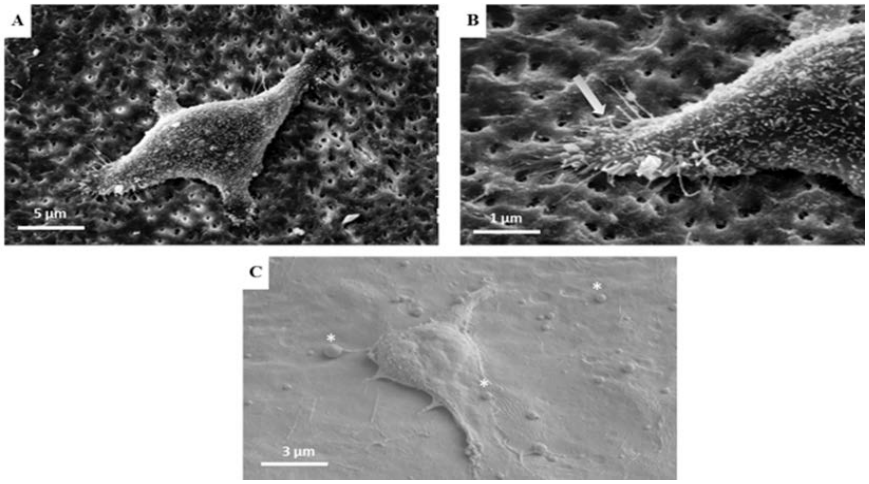

Figure 5: SEM of AM-hMSCs with CMSs at 14-21 days in vitro conditions. A. The AM-hMSCs showed fibroblastoid morphology and adhesion to the surface of CMSs at 14 days. B. The AM-hMSCs showed lamellipodia form (arrow) in contact to CMSs at 14 days. C. Spherical macrovesicles (*) of AM-hMSCs in surface of CMSs at 21 days. A-B. Electron microscopy DSM-950 (Zeiss). C. Electron microscopy Evo 10 (Zeiss). A: 2000x, B: 5000x, C: 2840x.

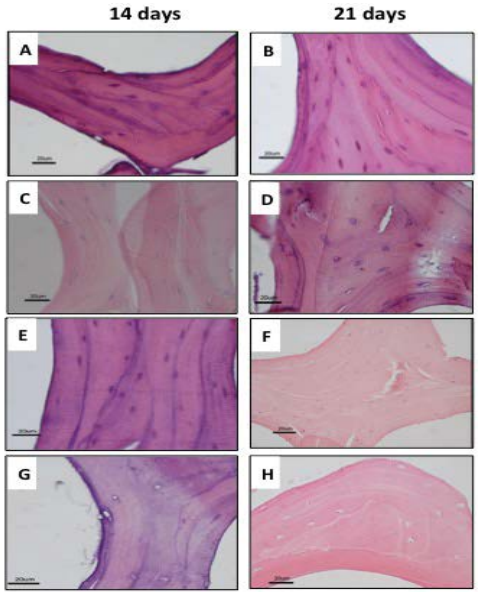

Figure 6: Microphotography of **CMSs** with AM-**hMSCs** at 14- and 21-days in vitro conditions. The AM-**hMSCs** seeded in CMSs stain with H&E at 14 days**(A)** and 21 days (B). Differentiation to chondroblast was confirm at 14 days **(C)** and 21 days **(D)** with stain Alcian blue. Osteoblast was observed at 14 days (E) and 21 days (F) with stain von Kossa, whereas adipocytes was present onto **CMSs** in 14 days (G) and 21 days (H) stain with oil red O. A-H: 20x

Discussion

In recent years, hMSCs have been considered an excellent option for the treatment of several diseases, as well as in the area of tissue regeneration. The differentiation capacity of hMSCs is known to be high, as is their capacity to regulate inflammatory processes, through the production and stimulation of multiple growth factors [5]. However, the protocols for hMSC procurement have not been fully standardized [23] and the administration routes and required doses have not been optimal or sufficient for reversing or decreasing organ damage [24].

The placenta is considered biologic waste and there are no ethical implications for its processing. The mother can donate it, by signing a statement of informed consent. We described herein a protocol for hMSCs procurement from the AM, according to ISTC established criteria, [25] as well as their biologic evaluation, with and without CMSs.

There were no differences in the biologic properties of AM-hMSCs obtained from natural delivery and cesarean sections. However, in in vitro cultures, the cells obtained from women ranging from 20-25 years of age displayed better proliferation and adaptation than those from older women (26 to 30 years of age). That could be correlated with the results of Alrefaei et al, who reported that MSCs from human fetal membrane (placenta, umbilical cord, and amniotic membrane) from older mothers (≥ 39) presented with short telomeres due to high telomerase activity [26].

Human MSCs from AM and BM were followed from passages P1 to P5, because Oja et al reported that P6 and subsequent passages from MSCs showed alterations in size, morphology, length of telomeres, and senescence evaluated in BM-hMSCs [22].

On the other hand, sox-2, oct-4, and nanog genes are well-established as being responsible for maintaining pluripotency in embryonic stem cells (ESCs) and MSCs, through self-renewal, and for suppressing differentiation-associated genes. The expression of sox-2 and oct-4 in AM-hMSCs showed no differences at any of the passages evaluated, suggesting that those cells conserve their stemness. However, oct-4 expression at P2 and P5 in the AM-hMSCs was higher than in the BM-hMSCs. We also found that nanog was downregulated in AM-hMSCs in P4 and P5. Moreover, nanog has been reported to be able to act independently from sox-2 and oct-4. In 2018, Akberdin et al suggested that sox-2 and oct-4 act as heterodimers that stimulate or inhibit pluripotential and differentiation genes [27]. Additionally, heterodimers could regulate nanog expression in MSCs derived from subcutaneous adipose tissue (hASCs). On the other hand, Pitrone et al demonstrated that knockdown of nanog inhibited the proliferation of hASCs, arresting the cell cycle in G0/G1 [28]. There is recently reported evidence that the expression of pluripotential genes is variable in spatiotemporal embryonic development and in the maintenance of MSC stemness. The triad of pluripotent genes in AM-hMSCs was observed, but future studies are needed to determine the specific regulatory network of those genes in AM-hMSCs.

The CD44, CD73, CD90, and CD105 surface markers were evaluated, according to the ISCT guidelines published in 2006 [25] We found that CD44, CD73, and CD90 in AM-hMSCs were similar in all the passages, compared with BM-hMSCs, with the exception of CD105, which displayed low levels in AM-hMSCs. In 2013, Leyva et al described two subpopulations of AM-hMSCs CD105+ and CD105- with dissimilar osteogenic potential. The CD105- cells showed stronger expression of secreted protein acidic and were rich in cysteine (SPARC), which was associated with more effective calcium deposition than in the CD105+ cells. Additionally, those authors reported that chondrogenic and adipogenic differentiation capacity was not different in either CD105+ or CD105- [29]. In contrast, our results revealed the high capacity for chondrogenic and osteogenic differentiation, but less capacity to differentiate into the adipogenic lineage. However, we did not sort the AM-hMSCs. Papait also reported low levels of CD105 (54.88 ± 25.83) in AM-hMSCs that did not compromise the potential of MSCs [30]. In 2013, Lin reported that CD105+ expression was underestimated as a MSCs marker, due to the differences observed in the initial and late stages [31]. Furthermore, the variation of superficial antigens expressed in MSCs was dependent on the source, patient age, and procurement protocol [32]. It is necessary to continue analyzing the difference in adipogenic lineage.

Moraes et al and Uder et al demonstrated that 20-30% of hMSCs maintained their initial morphology and stemness in vitro [33, 34], and it is possible that those cells are in a quiescent state. Similarly, we found that CD44, CD73, CD90, CD105, and HSCs, in approximately 42, 56, 51, 0.1, and 2.7%, respectively, of the AM-hMSCs incubated in the different differentiation media, conserved the membrane stemness markers at day 21 (data not shown). It is also possible that the concentration of growth factors plays an important role in the percentage of differentiated cells. Future studies are needed to determine the ideal concentration of growth factors and other mediators in the cultures of AM-hMSCs in chondroblast, osteoblast, and adipocyte differentiation media.

Collagen type I protein plays an important role in cell differentiation by providing biologic signals to induce cell differentiation. Collagen has been employed as a gel or sponge to design scaffolds that maintain the self-renewal and multipotential differentiation capacity of ESCs and MSCs in vitro for up to 30 days [10]. Other experiments for evaluating different conformations of collagen type I were conducted with gel or decellularized solid organs (liver, heart, and kidney) [35]. In particular, MSC-derived extracellular vesicles (EVs) were encapsulated to increase retention, stability, and the release of vesicles, in an ischemic kidney mouse model. That procedure enabled renal tubular epithelial cell proliferation, renal cell apoptosis inhibition, and angiogenesis enhancement, as well as fibrosis amelioration. The decellularization process to obtain extracellular matrix is time-consuming, requires many reagents, and a high number of hMSCs or iPSCs are needed to be implanted into the scaffold, in the recellularization process [36].

Porosity (%) and pore size, form, and distribution are the important physical characteristics of scaffolds that promote growth, adhesion, cytokine-growth factor release, and hMSCs differentiation. In 2018, Bonarsevt et al reported that the synthetic scaffold poly (3-hydroxybutyrate) (PHB), with poly (ethylene glycol) (PEG) and uniform pore size (about 125 μm), did not support MSCs, whereas scaffolds with diverse pore sizes promoted stem cell growth. In the scaffolds with small pores (about 45 μm), MSCs growth was the lowest and cell growth suppression was only partially related to stem cell differentiation [37]. In contrast, our CMSs had heterogeneous pore sizes (150-350μm) and open pores with high porosity [20]. We believe those characteristics facilitated the growth and differentiation into chondroblasts, osteoblasts, and adipocytes of the AM-hMSCs with CMSs at days 14 and 21. Those physical characteristics also enabled the diffusion of nutrients, growth factors, oxygen, and other biologic components that promote angiogenesis and the migration of native cells toward the scaffolds.

Regarding the proliferation and adhesion of hMSCs to the scaffold surface, the need to add fibronectin and/or growth factors, such as Bone Morphogenetic Proteins (BMP) 2 and 7, has been reported [38]. Our results demonstrated that the adhesion of AM-hMSCs to the CMSs employed required no addition of any biologic component. In fact, the formation of lamellipodia and production of microvesicles in the AM-hMSCs in contact with CMSs were observed through SEM.

On the other hand, there is extensive evidence that MSCs do not induce antigenic reactions in in vitro and in vivo assays [39]. Likewise, the abovementioned collagen scaffolds have inductive and conductive properties, with no evidence of rejection in the animal models that have been studied [15,16]. That correlates with our results, in which the human cells (AM-hMSCs) grew and proliferated in bovine scaffolds, signifying it could be a good xenogenic combination. Currently, we are evaluating the preliminary studies on CMSs construct and their implantation in a rat model.

All in all, CMSs possess the physical and chemical characteristics for their use as biomaterials in tissue engineering, enabling the proliferation, adhesion, and differentiation of AM-hMSCs. Implantation could also stimulate angiogenesis and the bioinduction of AM-hMSCs differentiation. Those conditions are associated with the 3D structure of CMSs that mimic the extracellular matrix and the natural environment [40-42]. Therefore, that construct (CMS plus AM-hMSCs) offers a promising approach for future applications in regenerative medicine.

Conclusion

The procurement of human MSCs from amniotic membrane was easy and safe and the protocol could be employed in tissue engineering. We demonstrated that human MSCs seeded in xenogenic collagen matrix scaffolds showed adhesion and differentiation into chondroblasts, osteoblasts, and adipocytes, in differentiation media. The innovative construct described herein, could be a first step in developing an excellent alternative in Regenerative Medicine for patients with chronic diseases that need to recover their health through organ transplantation**.**

Conflicts of Interest

The authors declare that they have no competing or commercial interest.

Funding Statement

Supported by the National Council for Science and Technology (CONACyT), grant number SALUD-2016-272579 and PAPIIT-UNAM TA200515.

Acknowledgments

Benjamín León-Mancilla is a doctoral student from the Programa de Doctorado en Ciencias Biomédicas, Universidad Nacional Autónoma de México (UNAM) and has receiver a DGAPA fellowship. We greatly appreciate the technical and ongoing support of MD Julia Antonio, MD Guillermo Ramirez and MD Martha Zancatl (Gynecology and Obstetric Services, Hospital General de México), Dr. Armando Pérez T., MS. Evelyn Pulido C., Chem. Verónica Rodríguez M., Biol. Armando Zepeda R., and Biol. Francisco Pasos N., (Department of Tissue and Cell Biology, Faculty of Medicine, UNAM); Marco Gudiño Z and Jaime Sánchez (Unit of Experimental Medicine; School of Medicine, Universidad Nacional Autónoma de México, UNAM. Hospital General de México) Dr. David Giraldo G., MS Irma López M.; Biol. Ivonne Sánchez C. (Microscopy Unit, Faculty of Medicine, UNAM). Dr. Ana Alfaro. (Pathology Service, Hospital General de México). Tech. Martina Flores., and Chem. Carlos Montoya (Oncology Hospital, IMSS).

References

1. World Health Organization (WHO) 2020.
2. Contreras AG (2016) Organ Tranplastation in Mexico. Transplantation, 100(10): 2011-2012.
3. Global Observatory on Donation and Transplantation (GODT) 2020.
4. Pereira MR, Mohan S, Cohen DJ, Husain SA, Dube GK, et al. (2020) COVID-19 in solid organ transplant recipients: Initial report from the US epicenter. Am J Transplant, 20(7):1800-1808.
5. Zhang H, Dai H, Xie X (2020) Solid organ transplantation during the COVID-19 pandemic. Frontiers in immunology. 11:1392.
6. Langer R, Vacanti J (1993) Tissue Engineering. Science. 260(5110):920-926.
7. Langer R, Langer L, Vacanti J (2014) Principles of Tissue Engineering. 4ed. Amsterdam: Elsevier.
8. Pham VP (2016) Stem Cell Processing. Switzerland: Springer.
9. Lim J, Razi ZR, Law J, Nawi AM, Idrus RB (2016) MSCs can be differentially isolated from maternal, middle and fetal segments of the human umbilical cord. Cytotherapy, 18(12):1493-1502.
10. Chien CC, Yen BL, Lee FK, Lai TH, Chen YC, et al. (2006) In vitro differentiation of human placenta-derived multipotent cells into hepatocyte-like cells. Stem Cells. 24(7):1759-1768.
11. Montesinos JJ, Flores-Figueroa E, Castillo-Medina S, Flores-Guzman P, Hernandez-Estevez E, et al. (2009) Human mesenchymal stromal cells from adult and neonatal sources: comparative analysis of their morphology, immunophenotype, differentiation patterns and neural protein expression. Cytotherapy, 11(2):163-176.
12. Badylak SF (2007) The extracellular matrix as a biologic scaffold material. Biomaterials, 28(25):3587-3593.
13. Freedman BR, Mooney DJ (2019) Biomaterials to mimic and heal connective tissues. Adv Mater, 31(19):e1806695.
14. Meyer M (2019) Processing of collagen based biomaterials and the resulting materials properties. Biomed Eng, 18:1-24.
15. Acevedo GC (2011) Xenoimplante de colágena en uretra de perro. Mexico City: Universidad Nacional Autónoma de México.
16. Montalvo-Jave EE, Mendoza Barrera GE, Valderrama Trevino AI, Pina Barba MC, Montalvo-Arenas C, et al. (2015) Absorbable bioprosthesis for the treatment of bile duct injury in an experimental model. Int J Surg, 20:163-169.
17. Mazza G, De Coppi P, Gissen P, Pinzani M (2015) Hepatic regenerative medicine. J Hepatol, 63(2):523-524.
18. Rodriguez-Fuentes N, Rodriguez-Hernandez AG, Enriquez-Jimenez J, Alcantara-Quintana LE, Fuentes-Mera L et al. (2013) Nukbone(R) promotes proliferation and osteoblastic differentiation of mesenchymal stem cells from human amniotic membrane. Biochem Biophys Res Commun, 434(3):676-80.
19. Li Y, Wu Q, Wang Y, Li L, Chen F, et al. (2017) Construction of bioengineered hepatic tissue derived from human umbilical cord mesenchymal stem cells via aggregation culture in porcine decellularized liver scaffolds. Xenotransplantation, 24(1): 1-15.
20. León-Mancilla BH, Araiza-Téllez MA, Flores-Flores JO, Piña-Barba MC (2016) Physico-chemical characterization of collagen scaffolds for tissue engineering. J Appl Res Tech. 14:77-85.
21. Vazquez NG, Echeverria O (2000) Introduction to electron microscopy applied to biological sciences. Mexico City: Economic Culture Fund, 168.
22. Oja S, Komulainen P, Penttila A, Nystedt J, Korhonen M (2018) Automated image analysis detects aging in clinical-grade mesenchymal stromal cell cultures. Stem Cell Res Ther, 9: 1-6.
23. Gnecchi M (2016) Mesenchymal stem cells. Methods and protocols. Methods in molecular biology. 2ed. New York: Humana Press.
24. Nicolas CT, Hickey RD, Chen HS, Mao SA, Lopera HM, et al. (2017) Concise review: Liver regenerative medicine: From hepatocyte transplantation to bioartificial livers and bioengineered grafts. Stem Cells, 35(1):42-50.
25. Dominici M, Le Blanc K, Mueller I, Slaper-Cortenbach I, Marini F, et al. (2006) Minimal criteria for defining multipotent mesenchymal stromal cells. The International Society for Cellular Therapy position statement. Cytotherapy, 8(4):315-317.
26. Alrefaei GI, Alkarim SA, Abduljabbar HS (2019) Impact of mothers' age on telomere length and human telomerase reverse transcriptase expression in human fetal membrane-derived mesenchymal stem cells. Stem Cells Dev, 28(24):1632-1645.
27. Akberdin IR, Omelyanchuk NA, Fadeev SI, Leskova NE, Oschepkova EA, et al. (2018) Pluripotency gene network dynamics: System views from parametric analysis. PLoS One, 13(3):e0194464.
28. Pitrone M, Pizzolanti G, Coppola A, Tomasello L, Martorana S, et al. (2019) Knockdown of NANOG reduces cell proliferation and Induces G0/G1 cell cycle arrest in human adipose stem cells. Int J Mol Sci. 20(10): 1-12.
29. Leyva-Leyva M, Barrera L, López-Camarillo C, Arriaga-Pizano L, Orozco-Hoyuela G, et al. (2013) Characterization of mesenchymal stem cell subpopulations from human amniotic membrane with dissimilar osteoblastic potential. Stem Cells Dev, 22(8):1275-1287.
30. Papait A, Vertua E, Magatti M, Ceccariglia S, De Munari S, et al. (2020) Mesenchymal stromal cells from fetal and maternal placenta possess key similarities and differences: Potential implications for their applications in regenerative medicine. Cells, 9(1): 1-23.
31. Lin CS, Xin ZC, Dai J, Lue TF (2013) Commonly used mesenchymal stem cell markers and tracking labels: Limitations and challenges. Histol Histopathol, 28(9):1109-16.
32. Naji A, Eitoku M, Favier B, Deschaseaux F, Rouas-Freiss N, et al. (2019) Biological functions of mesenchymal stem cells and clinical implications. Cell Mol Life Sci. 76(17):3323-3348.
33. Moraes DA, Sibov TT, Pavon LF, Alvim PQ, Bonadio RS, et al. (2016) A reduction in CD90 (THY-1) expression results in increased differentiation of mesenchymal stromal cells. Stem Cell Res Ther, 7:1-14.
34. Uder C, Bruckner S, Winkler S, Tautenhahn HM, Christ B (2018) Mammalian MSC from selected species: Features and applications. Cytometry A. 93(1):32-49.

35. Yang W, Xia R., Zhang Y, Zhang H, Bai L (2017) Decellurized liver scaffold for liver regeneration Methods in Molecular Biology, 1577:11-23.

36. Wang RM, Christman KL (2016) Decellularized myocardial matrix hydrogels: In basic research and preclinical studies. Advanced drug delivery reviews, 96:77-82.

37. Bonartsev AP, Zharkova II, Voinova VV, Kuznetsova ES, Zhuikov VA, et al. (2018) Poly(3-hydroxybutyrate)/poly(ethylene glycol) scaffolds with different microstructure: the effect on growth of mesenchymal stem cells. 3 Biotech, 8(8):1-10.

38. Ramalho L, Nedjari S, Guarino R, Awaja F, Gugutkov (2020) Fibronectin/ thermo-responsive polymer scaffold as a dynamic ex vivo niche for mesenchymal stem cells. J Mater Sci Mater Med, 31(12):129.

39. Fath-Bayati L, Ai J (2020) Assessment of mesenchymal stem cell effect on foreign body response induced by intraperitoneally implanted alginate spheres. J biol materials res Part A, 108(1):94-102.

40. Florian B, Michel K, Steffi G, Nicole H, Frant M, et al. (2019) MSC differentiation on two-photon polymerized, stiffness and BMP2 modified biological copolymers. Biomed Mater. 14: 1-13.

41. Ong CS, Yesantharao P, Huang CY, Mattson G, Boktor J, et al. (2018) 3D Bioprinting using Stem Cells. Pediatric Research.:1-23.

42. Somaiah C, Kumar A, Mawrie D, Sharma A, Patil SD, et al. (2015) Collagen Promotes Higher Adhesion, Survival and Proliferation of Mesenchymal Stem Cells. PLoS One, 10(12):e0145068.

Author Affiliations

Top

[1]*Liver, Pancreas and Motility (HIPAM) Laboratory; Unit of Experimental Medicine; School of Medicine, Universidad Nacional Autónoma de México, UNAM. Hospital General de México*

[2]*Department of Gynecology and Obstetric Services, Hospital General de México. "Dr. Eduardo Liceaga", Mexico City, Post code 06726, Mexico City, Mexico*

[3]*Department of Oncology Research Unit, Oncology Hospital, Instituto Mexicano del Seguro Social, National Medical Center, IMSS, Post code 06720, Mexico City, México*

[4]*Department of Materials Research Institute, Universidad Nacional Autónoma de México, Post code 04950, Mexico City, Mexico*

[5]*Department of Surgery, Laboratory Regenerative Medicine, Faculty of Medicine, Universidad Nacional Autónoma de México, Post code 04950, Mexico City, Mexico*